Aalborg Universitet

AALBORG UNIVERSITY
DENMARK

Selective Integration in the Material-Point Method

Andersen, Lars; Andersen, Søren; Damkilde, Lars

Published in:
Proceedings of the Twenty Second Nordic Seminar on Computational Mechanics

Publication date:
2009

Document Version
Publisher's PDF, also known as Version of record

[Link to publication from Aalborg University]

Selective Integration in the Material-point Method

Lars Andersen[*]**, Søren M. Andersen and Lars Damkilde**

Department of Civil Engineering
Aalborg University, Aalborg, Denmark
e–mail: la@civil.aau.dk

Summary The paper deals with stress integration in the material-point method. In order to avoid parasitic shear in bending, a formulation is proposed, based on selective integration in the background grid that is used to solve the governing equations. The suggested integration scheme is compared to a traditional material-point-method computation in which the stresses are evaluated at the material points. The deformation of a cantilever beam is analysed, assuming elastic or elastoplastic material behaviour.

Introduction

The material-point method (MPM) was proposed by Sulsky and coworkers [1, 2] as an alternative to the finite-element method (FEM) for analysis of problems in solid mechanics. The MPM can be described as a variation of the FEM, in which the material and any state variables are tracked at a finite set of material points that are allowed to move through a background grid of finite elements or cells. In contrast to a Lagrangian finite-element scheme, this allows the simulation of solids undergoing extreme deformation and displacements without mesh entanglement. Further, since the material follows the material points, mass diffusion occurring in Eulerian descriptions is avoided. Finally, the MPM automatically accounts for the exchange of momentum between adjacent bodies by solving the governing equations of motion a the nodes of the background grid.

Hence, apparently the MPM is useful for the analysis of problems in solid mechanics in which huge displacements and interaction between colliding bodies must be accounted for. However, in a standard MPM formulation, the stresses are evaluated at the material points. This may lead to *grid-crossing errors* as well as *parasitic shear*, in particular when linear interpolation functions are employed within the background grid.

Grid-crossing errors occur when a material point moves from one cell to another in a time step. This changes the sign of the stress contribution from that material point to the interior force at the adjacent grid nodes. As described by Bardenhagen et al. [3] this problem may be solved to some extent by smearing out the mass associated with a material point, leading to the so-called generalised-interpolation material-point (GIMP) method. Alternatively, higher-order interpolation may be applied as proposed by Andersen and Andersen [5].

Parasitic shear was reported by Cook et al. [4] in relation to linear quadrilateral elements applied to the analysis of bending. Thus, for first-order shape functions, the shear strains and stresses are only defined correctly at the centre of the element. Hence, full integration with two Gauss points in each direction may cause shear locking in bending. A similar effect occurs in the MPM since the material points are generally not placed at the centre of the computational cells. As described in this paper, it may therefore be advantageous to apply an integration scheme in the MPM corresponding to selective integration in the FEM.

Stress integration in the material-point method

The material-point method builds on the weak formulation. For the solid domain, Ω,

$$\int_{\Omega} \rho \mathbf{w} \cdot \mathbf{a} \, dV = - \int_{\Omega} \nabla \mathbf{w} : \rho \boldsymbol{\sigma}^s \, dV + \int_{\partial \Omega_\tau} \mathbf{w} \cdot \boldsymbol{\tau} \, dS + \int_{\Omega} \rho \mathbf{b} \, dV, \qquad (1)$$

where $\mathbf{w} = \mathbf{w}(\mathbf{x},t)$ is the virtual field, $\mathbf{a} = \mathbf{a}(\mathbf{x},t)$ the material acceleration, $\rho = \rho(\mathbf{x},t)$ the mass density, $\boldsymbol{\sigma}^s = \boldsymbol{\sigma}^s(\mathbf{x},t)$ the specific stress, $\mathbf{b} = \mathbf{b}(\mathbf{x},t)$ the external body force field, and $\boldsymbol{\tau} = \boldsymbol{\tau}(\mathbf{x},t)$ signifies the surface traction on $\partial\Omega_\tau$ where mechanical boundary conditions are prescribed. Here, $\boldsymbol{\sigma}^s = \boldsymbol{\sigma}/\rho$ and $\boldsymbol{\tau} = \boldsymbol{\sigma} \cdot \mathbf{n}$ with $\mathbf{n}$ denoting the unit outward normal to the boundary of the domain.

The density field $\rho(\mathbf{x},t) = \sum_{p=1}^{N_p} M_p \delta(\mathbf{x} - \mathbf{x}_p)$ is employed, where M_p is the mass of material point number p, $p = 1, \ldots, N_p$, and $\mathbf{x}_p = \mathbf{x}_p(t)$ is its position. Further, linear interpolation within the computational background grid, discretization of time and lumping the mass at the grid nodes provide the following system of equations for node number i and time step k:

$$m_i^k \mathbf{a}_i^k = \boldsymbol{\tau}_i^k + \mathbf{b}_i^k - \sum_{p=1}^{N_p} M_p \boldsymbol{\sigma}_p^{s,k} \cdot \mathbf{G}_{ip}^k, \qquad m_i^k = \sum_{p=1}^{N_p} M_p \Phi_i(\mathbf{x}_p^k) \tag{2}$$

where, for example, m_i^k is the mass associated with node number i at time step k. The interpolation function belonging to node i is denoted $\Phi_i(\mathbf{x})$, and $\mathbf{G}_{ip}^k = \nabla\Phi_i(\mathbf{x})|_{\mathbf{x}=\mathbf{x}_p^k}$. The first two terms on the left of Eq. (2) are identified as the external force on the body, whereas the final term represents the internal forces. In each time step, the velocities at the material points and nodes are updated as

$$\mathbf{V}_p^{k+1} = \mathbf{V}_p^k + \Delta t \sum_{i=1}^{N_n} \mathbf{a}_i^k \Phi_i(\mathbf{X}_p^k), \qquad m_i^{k+1} \mathbf{v}_i^{k+1} = \sum_{p=1}^{N_p} M_p \mathbf{V}_p^{k+1} \Phi_{ip}(\mathbf{x}_p^k). \tag{3}$$

Subsequently, the strain increments at the material points are determined by

$$\Delta\boldsymbol{\varepsilon}_p^k = \frac{\Delta t}{2} \sum_{i=1}^{N_n} \left\{ \mathbf{G}_{ip}^k \mathbf{v}_i^{k+1} + (\mathbf{G}_{ip}^k \mathbf{v}_i^{k+1})^T \right\}, \tag{4}$$

and the stresses are updated by a constitutive law. Two schemes are now compared: (1) a computation based on a standard MPM approach with the strain increments provided by Eq. (4), and (2) an alternative scheme with $\mathbf{G}_{ip}^k$ replaced by $\mathbf{G}_{ic}^k = \nabla\Phi_i(\mathbf{x})|_{\mathbf{x}=\mathbf{x}_c}$ for the determination of the shear strain increments, whereas Eq. (4) without modification for the computation of the normal strains. In the second approach, $\mathbf{x}_c$ denotes the coordinates of the point at the centre of the cell in which the material point resides. Hence, scheme no. 2 corresponds to selective integration.

Analysis of a cantilever beam

A cantilever beam is analysed by the MPM method, employing the explicit scheme described in the previous section. The length is $L = 8$ m in the x-direction, the height is $H = 2$ m in the y-direction and the beam has a mass density of $\rho = 10$ kg/m^3. The mesh size is 0.5 m and 2×2 material points are employed within each cell. Over a period of 0.5 s the beam is subjected to an increasing body force in terms of gravity with the final acceleration 10 m/s^2 in the negative y-direction. After this, the external force is kept constant.

Firstly, the analysis is carried out for an elastic material with Young's modulus $E = 10$ MPa and Poisson's ratio $v = 0$. Figure 1 shows the the normal and shear stresses, σ_{xx} and σ_{xy} after $t = 1$ s for Schemes 1 and 2, i.e. with standard MPM stress evaluation or 'selective integration'. Parasitic shear is clearly identified for σ_{xy} and, to some extent, the equivalent Mises stress σ_e. On the other hand, selective integration provides a smooth shear stress variation without reducing the accuracy of the normal stresses. However, the development of the mechanical energy is almost the same and only small differences are present in the displacement obtained with Schemes 1 and 2.
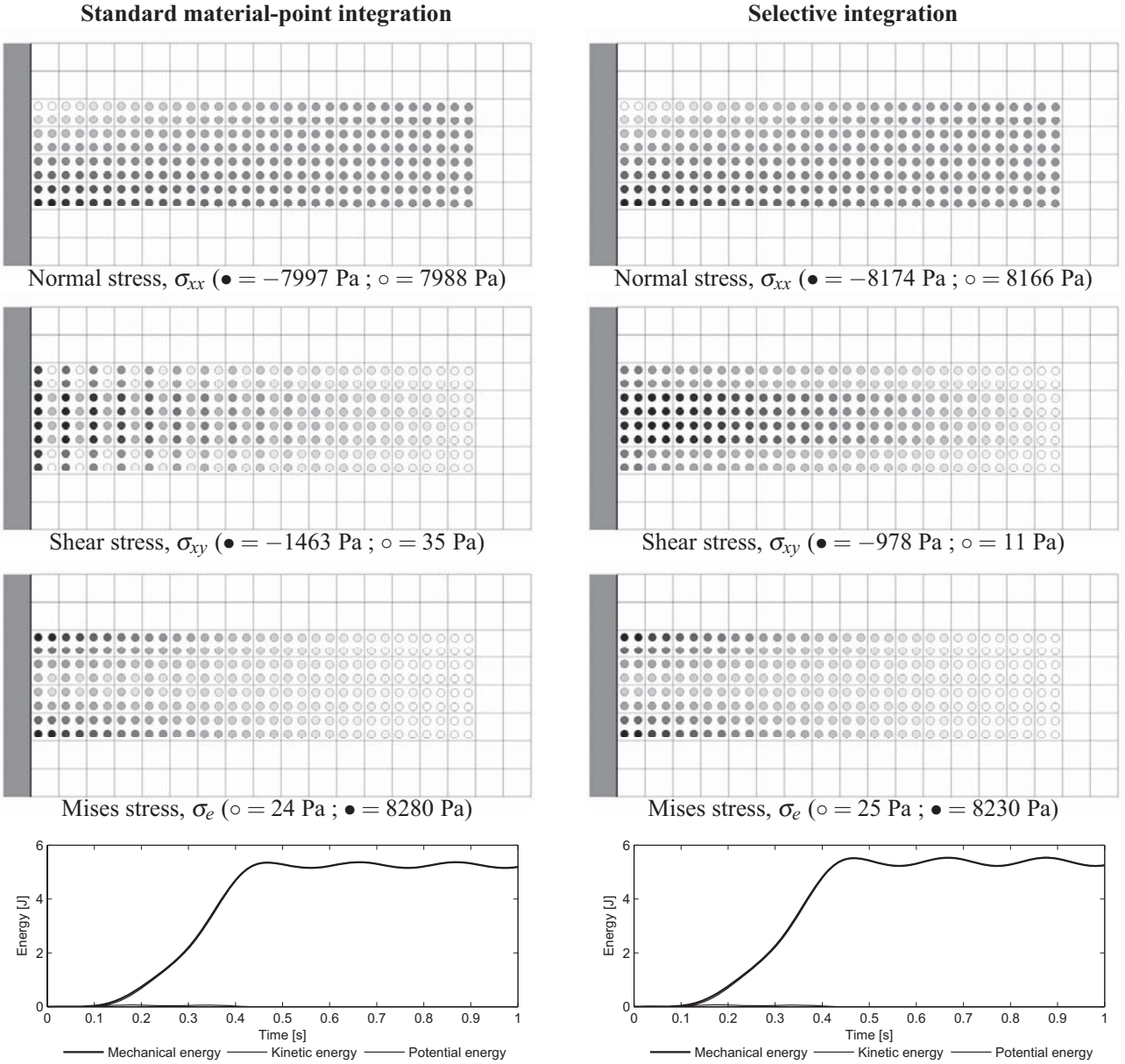
Standard material-point integration	Selective integration

Normal stress, σ_{xx} ($\bullet = -7997$ Pa ; $\circ = 7988$ Pa) | Normal stress, σ_{xx} ($\bullet = -8174$ Pa ; $\circ = 8166$ Pa)

Shear stress, σ_{xy} ($\bullet = -1463$ Pa ; $\circ = 35$ Pa) | Shear stress, σ_{xy} ($\bullet = -978$ Pa ; $\circ = 11$ Pa)

Mises stress, σ_e ($\circ = 24$ Pa ; $\bullet = 8280$ Pa) | Mises stress, σ_e ($\circ = 25$ Pa ; $\bullet = 8230$ Pa)

Figure 1: Stresses in the elastic beam at the end of the simulation.

The second analysis concerns a von Mises material with the yield criterion $f = \sigma_e - \sigma_0 \leq 0$, where σ_0 is the yield stress ($\sigma_0 = 4$ kPa in this analysis). Otherwise, the parameters are the same as before. The results are illustrated in Fig. 2, and again parasitic shear occurs in the case of standard MPM integration of the stresses. Nonetheless, no significant change can be seen in the extent and shape of the plastified zone. This is likely a result of the fact that $\sigma_{xx} \gg \sigma_{xy}$ in the present case.

Concluding remarks

Selective integration in the material-point method provides a better approximation of the shear stress distribution in a beam subjected to bending than standard MPM analysis with shear stress evaluation at the material points. Nonetheless, for beams with a length-to-height ratio of more than 4, standard MPM integration does not degenerate the solution for plastic problems since the axial normal stresses are dominating in bending. However, for other classes of problems in which shear stresses dominate, selective integration may be necessary in order to have a physically sound transition from elastic into plastic response.
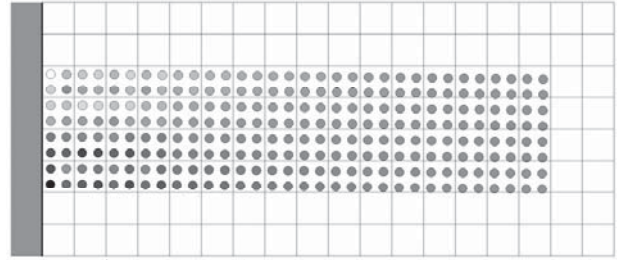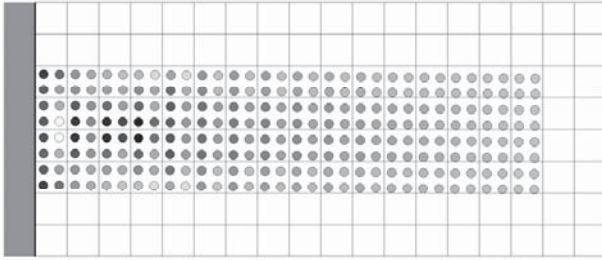
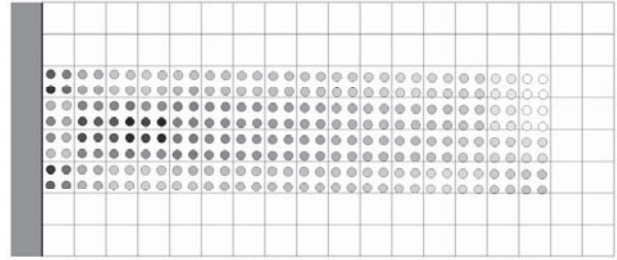**Standard material-point integration** **Selective integration**
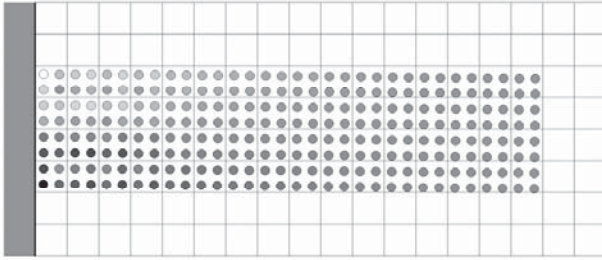
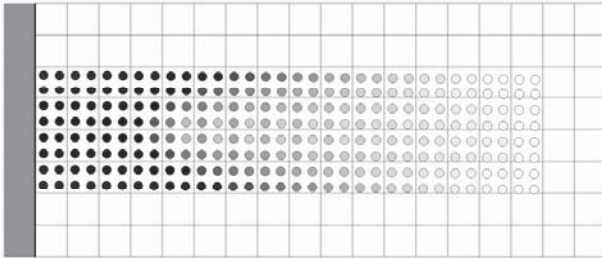Normal stress, σ_{xx} ($\bullet = -12151$ Pa ; $\circ = 12051$ Pa) Normal stress, σ_{xx} ($\bullet = -13192$ Pa ; $\circ = 13094$ Pa)
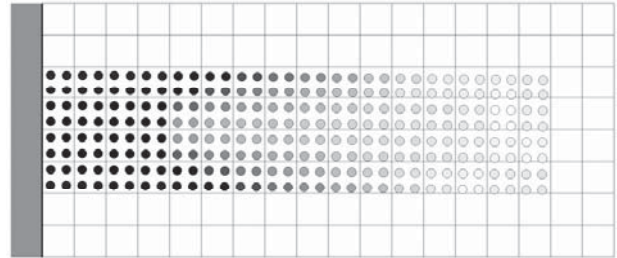
Shear stress, σ_{xy} ($\bullet = -1916$ Pa ; $\circ = 715$ Pa) Shear stress, σ_{xy} ($\bullet = -1666$ Pa ; $\circ = 245$ Pa)

Mises stress, σ_e ($\circ = 22$ Pa ; $\bullet = 3965$ Pa) Mises stress, σ_e ($\circ = 72$ Pa ; $\bullet = 3989$ Pa)
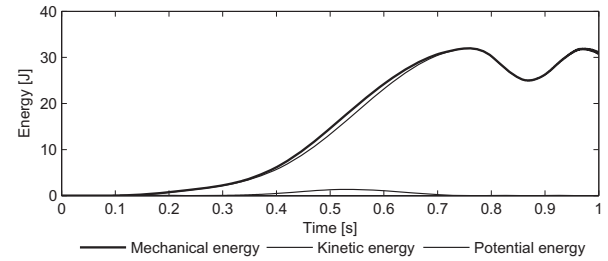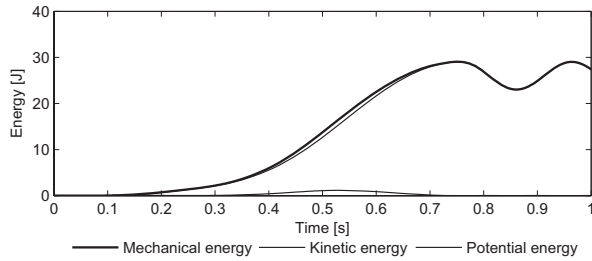
Figure 2: Stresses in the elastic-plastic beam at the end of the simulation.

References

[1] D. Sulsky, Z. Chen and H.L. Schreyer. A particle method for history-dependent materials. *Computer Methods in Applied Mechanics and Engineering*, **118**, 179–196, (1994).

[2] D. Sulsky, S.J. Zhou and H.L. Schreyer. Application of a particle-in-cell method to solid mechanics. *Compter Physics Communications*, **87**, 236–252, (1995).

[3] S.G. Bardenhagen and E.M. Kober. The generalized interpolation material point method. *Computer Modeling in Engineering and Sciences*, **5**(6), 477–495, (2004).

[4] R.D. Cook, D.S. Malkus and M.E. Plesha. *Concepts and Applications of Finite Element Analysis*. John Wiley & Sons, New York, Third edition, (1989).

[5] S.M. Andersen and L. Andersen. Material-Point Method Analysis of Bending in Elastic Beams. In *Proceedings of the Eleventh International Conference on Civil, Structural and Environmetal Engineering Computing*. Civil-Comp Press, Stirlingshire, Scotland, (2007).